

Preparation of Antibacterial PDMAEMA-Functionalized Multiwalled Carbon Nanotube via Atom Transfer Radical Polymerization

Young Tae Joo,¹ Kwang Ho Jung,¹ Min Joo Kim,¹ Yangsoo Kim^{1,2}

¹Department of Nano Systems Engineering, Inje University, Gimhae 621-749, Korea

²High Safety Vehicle Core Technology Research Center, Inje University, Gimhae 621-749, Korea

Correspondence to: Y. Kim (E-mail: cheykim@inje.ac.kr)

ABSTRACT: Poly[2-(dimethylamino)ethyl methacrylate] (PDMAEMA) was grafted onto the bromine-functionalized multiwalled carbon nanotubes (MWNTs) by applying an atom transfer radical polymerization (ATRP). The PDMAEMA-functionalized MWNT was characterized by Fourier transform infrared, transmission electron microscopy, Raman spectroscopy, thermal gravimetric analysis, and four-probe resistivity meter. The wt % of PDMAEMA present in the PDMAEMA-functionalized MWNT was estimated by applying the thermogram results for thermal gravimetric analysis. Variations of PDMAEMA content in the PDMAEMA-functionalized MWNT were tried by changing the ATRP process conditions such as the type of ligand and copper complex, the amount of DMAEMA based on the weight of bromine-functionalized MWNT, and the polymerization temperature. The phase behavior of PDMAEMA-functionalized MWNT in water depending on temperature and pH value was analyzed, and the PDMAEMA-functionalized MWNT showed the amphiphathic nature. The PDMAEMA-functionalized MWNT clearly showed an antibacterial effect against *E. coli* as well as *S. aureus*. The highest viability loss of *E. coli* achieved in this study was $\sim 42\%$ with the PDMAEMA-functionalized MWNT containing 53.9 wt % of PDMAEMA. The PDMAEMA-functionalized MWNT showed sheet resistance less than $\sim 9.68 \times 10^3 \Omega/\text{sq}$. © 2012 Wiley Periodicals, Inc. *J. Appl. Polym. Sci.* 000: 000–000, 2012

KEYWORDS: ATRP; PDMAEMA; MWNT; antibacterial effect; Raman spectroscopy

Received 4 July 2011; accepted 23 February 2012; published online

DOI: 10.1002/app.37571

INTRODUCTION

Carbon nanotubes (CNTs) have gained great importance on account of their outstanding mechanical, electrical, and thermal properties in the wide range of potential application areas such as organic electronics, materials science, and nanobiotechnology. Nevertheless, the major drawback of CNTs is that they characteristically show an aggregation owing to strong internanotube van der Waals interactions among them, which are ascribed to their characteristic high-aspect ratio and extended π -conjugated framework. The poor solubility due to the occurrence of CNT aggregation is to be suppressed in the preparation of hybrid polymeric materials containing CNTs as filler to synergistically improve their mechanical and electrical properties. An active research effort to resolve the aggregation problem in CNTs has been carried out, and a noticeable approach is a modification of CNTs with polymers. There are a couple of publications thoroughly reviewed regarding the chemical strategies for grafting polymer onto CNTs for the preparation of hybrid CNT/polymer composites.^{1,2} The covalent chemical bonding (grafting) of polymer to CNTs allows strong chemical bonds between CNTs

and polymer although it weakens the excellent properties of CNTs because of destroying the conjugated system of the CNT sidewalls. There have been two known methodologies (“grafting to” and “grafting from” approaches) for grafting polymer onto CNTs depending on how to chemically bond polymer chains to CNTs.¹ The “grafting to” approach involves beforehand a synthesis of a polymer having a specific molecular weight terminated with reactive groups or radical precursor. In a subsequent reaction, the polymer chain could be attached to the surface of CNTs by free-radical addition reactions. The “grafting from” approach involves growing polymer from the CNT surface, in which chemical species immobilized on the CNT sidewalls and edges initiated the polymerization of monomer. The “grafting from” approach has the merit of high-grafting efficiency, and another interesting advantage is that the polymer growth is not limited by steric hindrance. The atom transfer radical polymerization (ATRP) draws wide attention among the several “grafting from” processes, because it allows for the preparation of CNTs covalently modified by the polymers with interesting functionalities and architectures.

© 2012 Wiley Periodicals, Inc.

The newly discovered property of CNTs is an antibacterial activity. It has been reported that CNT itself^{3–5} as well as functionalized CNTs^{6–8} show an antibacterial effect against *Escherichia coli* (*E. coli*) and *Staphylococcus aureus* (*S. aureus*). Because of their high stability and low-environmental impact, antibacterial polymers have received increasing attention in fields such as hospital and dental equipment, water purification system, food packaging, and general consumer markets.⁹ Of specific attention polymer is poly[2-(dimethylamino)ethyl methacrylate] (PDMAEMA), and its antibacterial effect was reported in several recent publications.^{10–13} PDMAEMA shows an effective antibacterial effect against Gram-negative bacteria such as *E. coli* and *salmonella* and Gram-positive bacteria such as *S. epidermidis* and *S. aureus*.¹³ PDMAEMA is known to be a mucoadhesive polymer showing that it is cationic in acidified media or when quaternized with an alkylating agent.¹² It has also been known that PDMAEMA is an amphibious polymer,¹⁴ both pH- and temperature-sensitive,^{15–17} and it shows a lower critical solution temperature (LCST) behavior with phase separation at increased temperatures.¹⁷

There have been published several remarkable reports regarding the modified multiwalled carbon nanotubes (MWNTs) prepared by grafting PDMAEMA onto the functionalized MWNT via ATRP.^{18–21} Hu et al.¹⁸ achieved the preparation of PDMAEMA brushes formed on MWNT by applying ATRP with polydopamine-modified MWNT. Quaternized-PDMAEMA brushes (Q-PDMAEMA) were obtained by subsequent quaternization process, and then palladium nanoparticles were attached onto the Q-PDMAEMA. Priftis et al.¹⁹ reported the ATRP of 2-(dimethylamino)ethyl methacrylate (DMAEMA) in the presence of macroinitiators based on the bromine-functionalized MWNT, which were prepared by using the series reaction processes such as Diels–Alder cycloaddition reaction, surface initiated anionic or ring opening polymerization, and bromine group attachment reaction. Gao et al.²⁰ and Li et al.²¹ characterized PDMAEMA-grafted MWNT prepared by *in situ* ATRP of DMAEMA in the presence of bromine group attached MWNT. The nanohybrid materials were successfully obtained by loading CdTe quantum dots and Fe₃O₄ magnetic nanoparticles onto the surface of PDMAEMA-grafted MWNT by electrostatic self-assembly method.

Several reports on the PDMAEMA-functionalized MWNT prepared by applying the physical interactions alone without any *in situ* grafting reaction are also noted.^{22,23} The functionalized MWNT prepared by applying the cation– π interactions between PDMAEMA and MWNT showed a pH-dependent solubility caused by the presence of a noncovalently bonded PDMAEMA.²² The layer-by-layer-structured MWNT-PDMAEMA–PSS-PDMAEMA was prepared by applying the alternating electrostatic interaction with the functionalized MWNT as template, which was obtained by an acid treatment or grafting anionic polyelectrolyte.²³

In this study, the PDMAEMA-functionalized MWNT was prepared by applying the ATRP of DMAEMA on the surface of bromine-functionalized MWNT (“grafting-from” approach).

The variations of ligand type, polymerization temperature, and the number of moles of DMAEMA added per unit weight (gram) of bromine-functionalized MWNT were tried in the ATRP of DMAEMA. The antibacterial effect against *E. coli* and *S. aureus*, the solubility in organic solvent and water, and the phase-separation behavior depending on temperature and pH value were investigated for the PDMAEMA-functionalized MWNT. The covalent bond formed between MWNT and PDMAEMA was also characterized by using Raman spectroscopy. To authors’ knowledge, none of the published works to date has reported an antibacterial effect for the PDMAEMA-functionalized MWNT. It was sought the preparation of the PDMAEMA-functionalized MWNT showing intrinsic properties pertaining to not only MWNT but also PDMAEMA. One of the potential applications using the PDMAEMA-functionalized MWNT is the mechanical reinforcements accompanying antibacterial effect through a facile compounding process with polymer matrix. The compounded polymeric materials would concomitantly show the electromagnetic interference (EMI) shielding or electrostatic dissipation (ESD) effect, because they contain MWNT showing electrical conductivity.

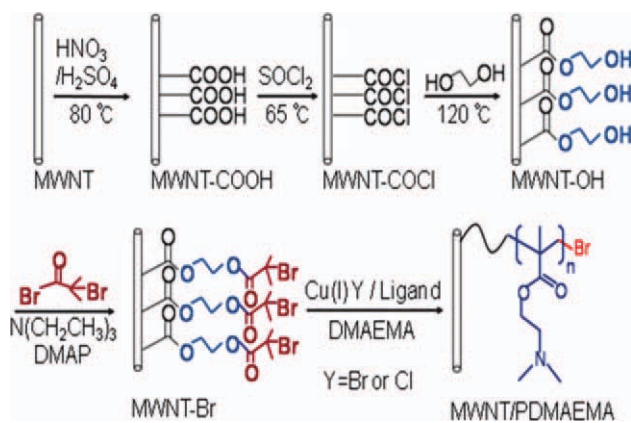
EXPERIMENTAL

Materials

MWNT (CM95) was purchased from Hanwha Nanotech (Korea). DMAEMA (98%, Aldrich) was purified by passing through an inhibitor remover column (Aldrich) before use. The following chemicals were used as received in this study: copper(I) chloride [Cu(I)Cl; $\geq 99\%$, Sigma-Aldrich], copper(I) bromide [Cu(I)Br; 98%, Aldrich], triethylamine ($\geq 99.5\%$, Sigma-Aldrich), 4-di(methylamino)pyridine ($\geq 99\%$, Aldrich), α -bromoisobutryl bromide (98%, Aldrich), bromoethane (98%, Sigma-Aldrich), ethylene glycol (99%, Katayama Chemical), acetonitrile (99%, Katayama Chemical), chloroform (CHCl₃; $\geq 99\%$, Aldrich), tetrahydrofuran (THF; $\geq 99\%$, Aldrich), nitric acid (HNO₃; 70%, Sigma-Aldrich), sulfuric acid (H₂SO₄; 95–98%, Sigma-Aldrich), and thionyl chloride (SOCl₂; Fluka). And tris(2-pyridylmethyl)amine (TPMA; 98%, Aldrich), tris[2-(dimethylamino)ethyl]amine (Me₆TREN; Aldrich), *N,N,N',N'*, *N''*-pentamethyldiethylenetriamine (PMDETA; 99%, Aldrich), 2,2'-bipyridine (bpy; $\geq 99\%$, Sigma-Aldrich), and 4,4'-di(5-nonyl)-2,2'-bipyridyne (dNbpy; 97%, Aldrich) were used without further purification, and either of them was used as a ligand in the preparation of the PDMAEMA-functionalized MWNT via ATRP. A technical-grade toluene, methanol, and acetone were also used in this study.

Preparation of the PDMAEMA-Functionalized MWNT

Bromine-functionalized MWNT (MWNT-Br) was used as an initiator in the ATRP, and it was obtained by the series reaction processes depicted in Scheme 1, which was based on the experimental procedure reported by Kong et al.²⁴ The MWNT having an acid functional group (MWNT-COOH), MWNT having a carbonyl chloride functional group (MWNT-COCl), MWNT having a hydroxyl functional group (MWNT-OH), and finally MWNT having a bromine functional group (MWNT-Br) were



Scheme 1. Stepwise preparation flows for the PDMAEMA-functionalized MWNT using a pristine MWNT as a starting material. [Color figure can be viewed in the online issue, which is available at wileyonlinelibrary.com.]

consecutively prepared with a pristine MWNT as a starting material.

Then, a “grafting-from” method via ATRP of DMAEMA was applied for the preparation of the PDMAEMA-functionalized MWNT. The MWNT-Br sample, toluene (70 mL/g of MWNT-Br), and copper complex (either Cu(I)Br or Cu(I)Cl; 2.0 mmol/g of MWNT-Br) and ligand (4.0 mmol/g of MWNT-Br) were poured into a round-bottomed flask in the atmosphere of nitrogen. Then, the reaction mixture was heated up to 60°C, and a specific amount of DMAEMA was added using a syringe in order to start an ATRP. After 20 h, the polymerization was stopped by adding THF, and then the mixture was filtered through 0.1 μm ADVANTEC® PTFE membrane filter, and it was repeatedly washed with THF to remove any free homopolymer in the product. The obtained solid was immersed into a copious amount of methanol, filtered, washed, and finally dried overnight in vacuum oven at 60°C.

Quaternization of the PDMAEMA-Functionalized MWNT

The PDMAEMA-functionalized MWNT was mixed with bromoethane/acetonitrile (1 : 2 in volume; 35.7 mL/g of PDMAEMA-functionalized MWNT) at 40°C. After 12 h, the solid product was recovered and washed with methanol, DI-water, and acetone in series.

Assessment of Antibacterial Effect for the Quaternization-Treated PDMAEMA-Functionalized MWNT

Both a pristine cellulose filter paper untreated and a cellulose filter paper coated with the quaternization-treated PDMAEMA-functionalized MWNT were immersed in a certain volume of Luria broth with *E. coli* (ATCC 29425) at 37°C for 24 h and then they were freeze-dried for overnight. Freeze-dried samples were transferred to the SEM analysis for the identification of *E. coli* present in the cellulose filter paper. A colony-forming unit (CFU) was estimated to measure an antibacterial activity against *E. coli* for the quaternization-treated PDMAEMA-functionalized MWNT. A colony of *E. coli* grown on an agar plate was added to a certain volume of Luria broth contained in a sterile tube,

and the culture was incubated at 37°C while being shaken at 45 rpm for 24 h. Then, the cells were highly diluted with sterile distilled water. A nutrient solution of prescribed composition containing bacto yeast (BD Bacto™), trypton (BD Bacto), NaCl, agar, and distilled water was prepared. A sonicated aqueous solution containing a certain amount of either the quaternization-treated PDMAEMA-functionalized MWNT or a pristine MWNT was prepared. Then, these two mixtures (nutrient solution and aqueous solution having either the quaternization-treated PDMAEMA-functionalized MWNT or a pristine MWNT) were blended together and sterilized in an autoclave at 121°C for 15 min. A certain volume of diluted cell-culture solution was added to the whole mixture with agitation at $\sim 40^\circ\text{C}$, and the resulting mixture was poured in the Petri dish and incubated at 37°C for 24 h. Finally, a CFU of the sample in agar plate was counted to measure a viability of *E. coli*.

Characterization of the PDMAEMA-Functionalized MWNT

Scanning electron microscope–energy-dispersive X-ray spectroscopy (SEM–EDX; HORIBA E-MAX X-treme) was used to identify the presence of functional groups (–Cl and –Br) in the MWNT-COCl and MWNT-Br samples. Fourier transform infrared (FTIR) spectroscopy analysis was carried out on the PDMAEMA-functionalized MWNT sample dispersed in KBr discs using a Varian Model Scimitar 1000. For the estimation of wt % of PDMAEMA in the PDMAEMA-functionalized MWNT, thermal gravimetric analysis (TGA) was carried out using a TA Instrument model TGA Q50 with a heating rate of 10°C/min under nitrogen atmosphere. For the identification of PDMAEMA, Raman spectra of the PDMAEMA-functionalized MWNT and a pristine MWNT were obtained on a HORIBA Jobin Yvon Model LabRAM HR 800 UV at 633 nm of laser excitation wavelength. Morphology of the PDMAEMA-functionalized MWNT was analyzed using a transmission electron microscopy (TEM) operating at 80 kV (Hitachi Model H-7500). For the preparation of TEM specimen, drops of the PDMAEMA-functionalized MWNT dispersed in DI-water were dried on a copper grid having a formvar/carbon support film. Samples for field emission-scanning electron microscopy (FE–SEM) analysis were coated with Pt/Pd by sputtering for 150 s. The FE–SEM images were obtained on a Hitachi Model S-4300SE operating at 15 kV. The sheet resistance was measured using a Mitsubishi Chemical Analytech Model Loresta-EP MCP-T360 four-probe resistivity meter at room temperature. For the preparation of sheet-resistance specimens, the vacuum-dried PDMAEMA-functionalized MWNT sample was comingled with a small portion of carboxymethyl cellulose (CMC; <5 wt %) in the presence of DI water and then ground with pestle in a mortar. The rectangular-shaped thin specimen with a dimension of 2.5 cm \times 2.5 cm was prepared by coating the PDMAEMA-functionalized MWNT slurry with a doctor blade. The specimen was dried under vacuum at 60°C for 24 h and then transferred for the sheet-resistance measurement. For the observation of phase behavior depending on the solvent type, temperature, and pH value, solution containing the PDMAEMA-functionalized MWNT was sonicated for 30 min, and then the visual observation was made.

RESULTS AND DISCUSSION

ATRP of DMAEMA Using MWNT-Br as an Initiator

Identification of PDMAEMA Present in the PDMAEMA-Functionalized MWNT. The bromine-functionalized MWNT (MWNT-Br) was used as a surface initiator for the ATRP of DMAEMA, and thus, PDMAEMA chains were grown in the initiating sites of MWNT-Br. Scheme 1 shows stepwise procedures for the preparation of PDMAEMA-functionalized MWNT, which starts from a pristine MWNT and ends in the PDMAEMA-functionalized MWNT. The functional groups of chlorine ($-\text{Cl}$) and bromine ($-\text{Br}$) introduced into MWNT were identified using SEM-EDX spectroscopy in our previous report.²⁵

Figure 1 shows the FTIR spectrum of PDMAEMA-functionalized MWNT (PDMAEMA 53.9 wt %) prepared by using a combination of Cu(I)Br and PMDETA as a catalytic system at 60°C of ATRP temperature. The characteristic peaks at 2924 and 2855 cm^{-1} are attributed to the methylene groups of grafted polymer chains, in particular to the asymmetrical and symmetrical stretching, respectively. Absorptions arising from C—H stretching of methyl groups occur at 2967 and 2870 cm^{-1} . The peak at 1726 cm^{-1} is due to the C=O stretch of ester group and 1150 cm^{-1} to the C—N stretching of $-\text{N}(\text{CH}_3)_2$ group, respectively. These characteristic peaks confirm the presence of PDMAEMA, and they agree with the observation by Yang et al.²⁶ The C=O stretching of the $-\text{COOH}$ group is also observed at 1635 cm^{-1} in Figure 1, and another wide absorption band corresponding to the OH stretching of $-\text{COOH}$ group, which is not presented in Figure 1, appears around 3400 cm^{-1} . These two characteristic peaks reveal the presence of carboxylic acid group in the PDMAEMA-functionalized MWNT. It seems that the conversion reaction of MWNT-COOH to MWNT-COCl sample is incomplete, and, thus, the acid ($-\text{COOH}$) group remains on the surface of MWNT.

Figure 2 shows TEM microphotographs of pristine MWNT [Figure 2(a)] and PDMAEMA-functionalized MWNT containing 24.8 wt % [Figure 2(b)] and 53.9 wt % [Figure 2(c)] of PDMAEMA. It shows that the diameters of PDMAEMA-functionalized MWNT (23.1–58.7 nm) were clearly increased compared to those of pristine MWNT (11.1–19.1 nm) due to the formation of PDMAEMA on the surface of MWNT.

Figure 3(a) shows the Raman spectra of pristine MWNT and PDMAEMA-functionalized MWNT (Cu(I)Br/PMDETA , 60°C , PDMAEMA 53.9 wt %). Raman spectrum of the pristine MWNT shows the characteristic peaks at 1320 and 1571 cm^{-1} corresponding to the D and G-band, respectively, which are attributed to the defects and disorder-induced modes and the tangential C—C bond-stretching motions. Compared to the pristine MWNT, the D-band of the PDMAEMA-functionalized MWNT shifts upward by 7 cm^{-1} from 1320 to 1327 cm^{-1} , and the G-band of them shifts upward by 12 cm^{-1} from 1571 to 1583 cm^{-1} . The D' -band, which is known to be directly affected by the disorder in MWNT, clearly appears at 1606 cm^{-1} for the PDMAEMA-functionalized MWNT; however, it is barely observable in pristine MWNT. Figure 3(b) illustrates the establishment of linear relationship between the wt % of PDMAEMA in the

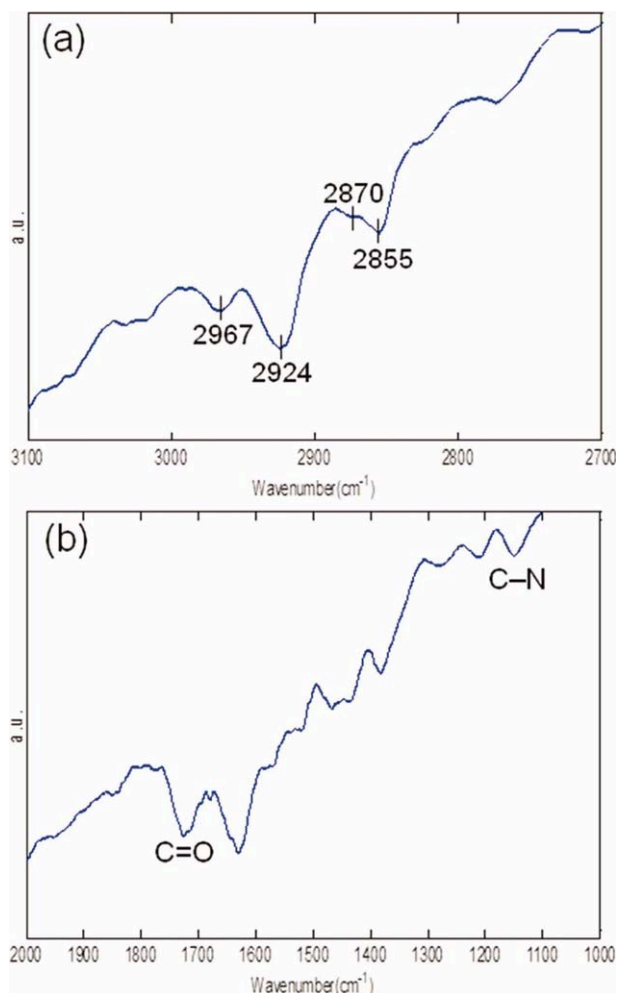


Figure 1. FTIR spectrum of the PDMAEMA-functionalized MWNT (Cu(I)Br/PMDETA and 60°C in ATRP; PDMAEMA 53.9 wt %). [Color figure can be viewed in the online issue, which is available at wileyonlinelibrary.com.]

PDMAEMA-functionalized MWNT and the relative intensity ratio of D to G band (I_D/I_G), which means that the Raman intensity ratio of D/G band proportionally increases with the content of polymer grafted on the surface of MWNT. These obvious changes in Raman spectrum of the PDMAEMA-functionalized MWNT indicate the formation of sp^3 -hybridized carbons on the PDMAEMA-grafted MWNT, which means a successful covalent bonding of PDMAEMA to the MWNT side walls. There are several reports, suggesting that the Raman signal of polymer-functionalized CNTs is strongly dependent on the grafted polymer species, and, thus, it can be taken as a measure of the degree of functionalization.^{27–30}

PDMAEMA Content and Thermal Weight Loss of the PDMAEMA-Functionalized MWNT Depending on the Process Conditions of ATRP. In the ATRP, a suitable ligand in combination with a transition metal complex establishes a reversible equilibrium between dormant species and active radical species, and it dissolves a copper complex and tunes the copper catalyst activity.³¹ ATRP allows a reduction of the concentration of

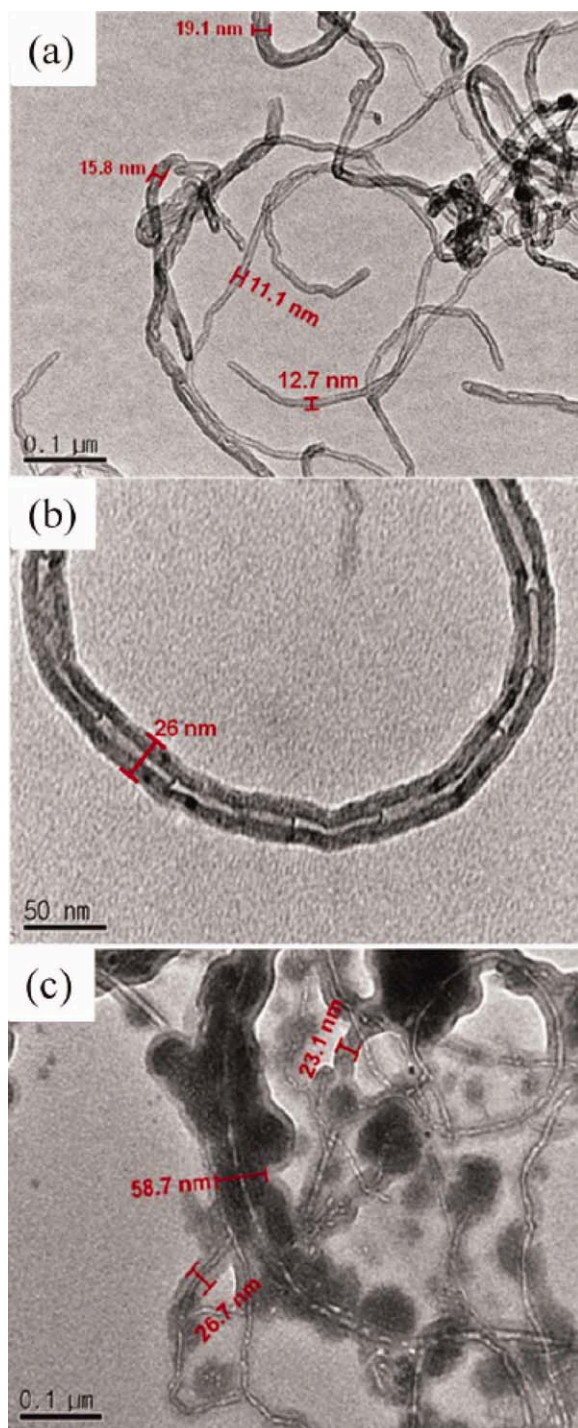


Figure 2. TEM microphotographs of (a) pristine MWNTs, (b) the PDMAEMA-functionalized MWNT containing 24.8 wt % of PDMAEMA, and (c) the PDMAEMA-functionalized MWNT containing 53.9 wt % of PDMAEMA (Cu(I)Br/PMDETA and 60°C in ATRP). [Color figure can be viewed in the online issue, which is available at wileyonlinelibrary.com.]

active radical species in the propagation step helping minimize the chance of termination reaction among the growing polymeric radicals, and, thus, it facilitates not only a control of polymer molecular weight and its polydispersity but also a

design of polymer molecular structure. In this study, a combination of one of the five types of nitrogen-based ligands (TPMA, Me₆TREN, PMDETA, bpy, and dNbpy) and a copper complex of either Cu(I)Br or Cu(I)Cl was used to prepare the PDMAEMA-functionalized MWNT via ATRP. Table I shows chemical structures of ligands and their respective reaction rate constants for the activation path defined in ATRP mechanism, which are excerpts from the report by Tang et al.³¹

Figure 4 shows TGA thermograms of PDMAEMA-functionalized MWNT [Figure 4(a)] and wt % of PDMAEMA in the PDMAEMA-functionalized MWNT [Figure 4(b)] depending on the number of moles of DMAEMA used in ATRP (Cu(I)Br/PMDETA, 60°C), numerical values of which are shown in Figure 4(a) and based on the unit weight of MWNT-Br used as an initiator. A thermal weight loss of the PDMAEMA-functionalized MWNT in TGA is correspondingly intensified with the additional use of DMAEMA. An overall weight loss of the PDMAEMA-functionalized MWNT in the TGA thermogram corresponds to the thermal decomposition of PDMAEMA. Therefore, the composition (W_{polymer} wt %) of PDMAEMA present in the PDMAEMA-functionalized MWNT can be estimated by using the following equation, in which $w_{\text{MWNT-Br}}$, $w_{\text{composites}}$, and w_{PDMAEMA} are the wt % values for MWNT-Br (79.9 wt %), the PDMAEMA-functionalized MWNT prepared in this study, and PDMAEMA (3.9 wt %) at 800°C in the TGA thermogram, respectively.

$$W_{\text{polymer}}(\%) = \frac{w_{\text{MWNT-Br}} - w_{\text{composites}}}{w_{\text{MWNT-Br}} - w_{\text{PDMAEMA}}} \times 100 \quad (1)$$

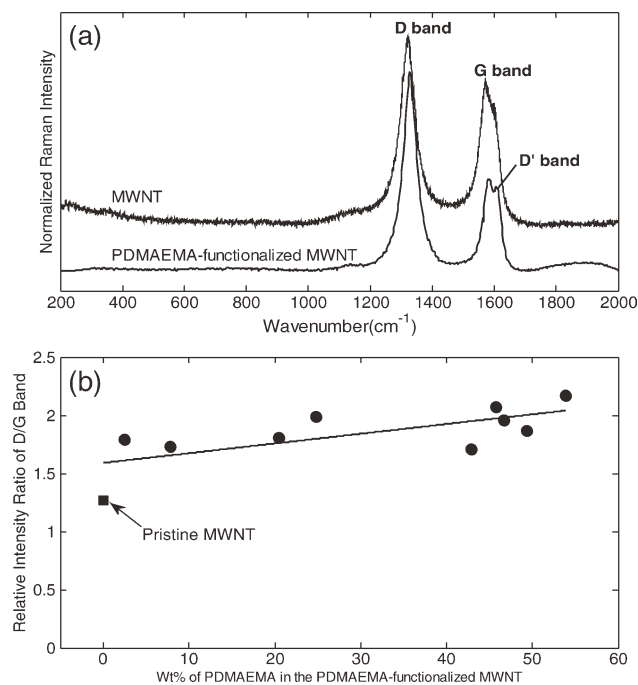


Figure 3. (a) Raman spectra of pristine MWNTs and the PDMAEMA-functionalized MWNT (Cu(I)Br/PMDETA and 60°C in ATRP; PDMAEMA 53.9 wt %) and (b) Raman intensity ratio of D/G band depending on the wt % of PDMAEMA in the PDMAEMA-functionalized MWNT (Cu(I)Br/PMDETA and 60°C in ATRP).

Table I. Chemical Structures and Activation Rate Constants of Ligands Used in the Preparation of PDMAEMA-Functionalized MWNT

Chemical structure	Name	k_{act} ($M^{-1} s^{-1}$) ³¹
	Tris[(2-pyridyl)methyl]amine (TPMA)	62
	Tris[2-(dimethylamino)ethyl]amine (Me ₆ TREN)	450
	N,N,N',N',N''-pentamethyldiethyl 2.7 enetriamine (PMDETA)	2.7
	2,2'-Bipyridine (bpy)	0.066
	4,4'-Di(5-nonyl)-2,2'-bipyridyne (dNbpy)	0.60

Figure 4(b) shows that the wt % of PDMAEMA in the PDMAEMA-functionalized MWNT linearly increases with the number of moles of DMAEMA added per unit weight (gram) of the MWNT-Br used in ATRP. A couple of published works

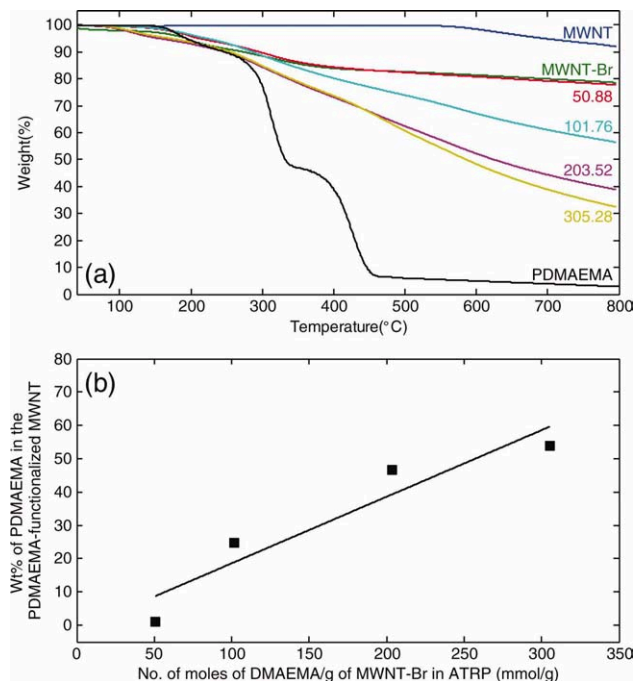


Figure 4. (a) TGA thermograms of the PDMAEMA-functionalized MWNT and (b) the wt % of PDMAEMA present in the PDMAEMA-functionalized MWNT depending on the number of moles of DMAEMA added per unit weight (gram) of MWNT-Br used in ATRP (Cu(I)Br/PMDETA and 60°C in ATRP). [Color figure can be viewed in the online issue, which is available at wileyonlinelibrary.com.]

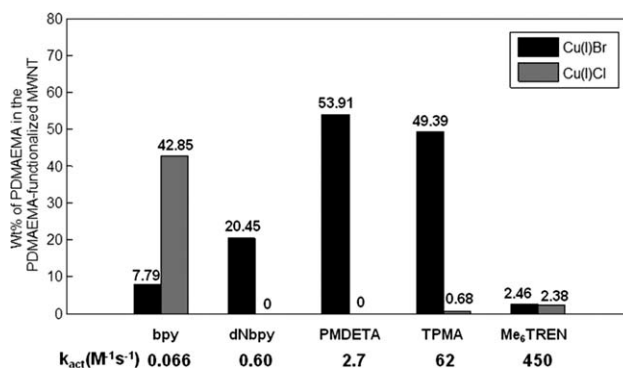


Figure 5. The wt % of PDMAEMA present in the PDMAEMA-functionalized MWNT depending on not only the type of copper complex and ligand but also the activation rate constant for ligand (60°C in ATRP).

show that there establishes a linear relationship between the amount of polymer grafted onto CNTs and the number of moles of monomer used in the preparation of the CNT/polymer nanocomposites via ATRP.^{21,24} The linearity between them clearly confirms a characteristic feature of the living controlled free radical polymerization, which is ATRP in this study.

Figure 5 shows that the wt % of PDMAEMA in the PDMAEMA-functionalized MWNT is greatly affected by not only a type of copper complex and ligand but also the activation rate constant for ligand. The highest yield of PDMAEMA in the preparation of PDMAEMA-functionalized MWNT via ATRP is provided with the selection of either Cu(I)Br/PMDETA or Cu(I)Cl/bpy system regarding a copper complex and a ligand in the ATRP. It clearly shows that when using Cu(I)Cl as a copper complex, a ligand (bpy) having the slowest activation rate constant ($0.066 M^{-1} s^{-1}$) needs to be combined with the copper complex for the preparation of PDMAEMA-functionalized MWNT having the highest polymer content. Meanwhile, in case of using Cu(I)Br as a copper complex, it needs to be chosen as an appropriate ligand showing the optimal activation rate constant, which is PMDETA in this study.

Figure 6 shows that in order to obtain the PDMAEMA-functionalized MWNT having the highest polymer content, the ATRP of DMAEMA needs to be carried out at the optimum

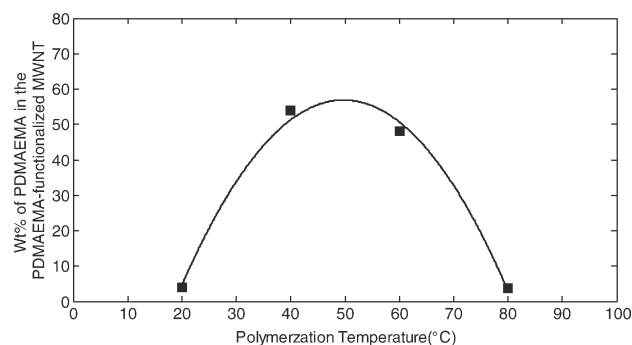


Figure 6. The wt % of PDMAEMA present in the PDMAEMA-functionalized MWNT depending on the ATRP temperature (Cu(I)Br/PMDETA).

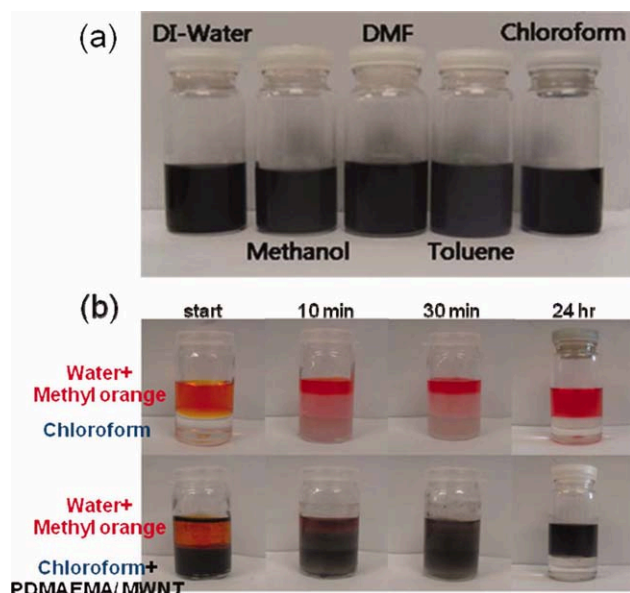


Figure 7. (a) Solubility in water and organic solvents and (b) amphipathic property test for the PDMAEMA-functionalized MWNT (Cu(I)Br/PMDETA and 60°C in ATRP; PDMAEMA 53.9 wt %). [Color figure can be viewed in the online issue, which is available at [wileyonlinelibrary.com](http://www.wileyonlinelibrary.com).]

polymerization, which is around 50°C for the catalytic system of Cu(I)Br/PMDETA. The highest composition of PDMAEMA in the PDMAEMA-functionalized MWNT was achieved at 53.9 wt % in this study, which corresponds to the degree of polymerization of 52 for PDMAEMA grafted onto the functionalized MWNT.

Characteristic Properties of the PDMAEMA-Functionalized MWNT

Phase behavior. According to the report by Duan et al.,¹⁴ PDMAEMA is dissolved in not only water having pK_a of 7.0 ± 0.5 but also most organic solvents except alkanes. Aqueous and organic solutions containing the PDMAEMA-functionalized MWNT were prepared in order to confirm its solubility in both water and organic solvents. Figure 7(a) shows that stable solutions without precipitation in both water and organic solvents (methanol, DME, toluene, chloroform) were maintained for more than 24 h. Figure 7(b) shows a phase-transfer behavior of the PDMAEMA-functionalized MWNT having an amphipathic nature. The solution composed of two separate layers of water, and chloroform was initially prepared (“start”) and then sonicated for 30 min. After sonication process, the solution was left as it was without agitation, and then the visual observation of phase transfer behavior was made with the lapse of time (10 min, 30 min, and 24 h). A phase behavior for the solution of water and chloroform without containing the PDMAEMA-functionalized MWNT was also presented in the upper images of Figure 7(b) for a comparison. Methyl orange was dissolved in water for coloring in order to be distinguishable from chloroform layer. The lower images show that there occurs a phase transfer of the PDMAEMA-functionalized MWNT from chloroform to the water layer following the sonication procedure. It

means that not only the PDMAEMA-functionalized MWNT is soluble in both chloroform and water but also it prefers to reside in water rather than chloroform. It is highly probable that the presence of acid ($-\text{COOH}$) group in the PDMAEMA-functionalized MWNT (Figure 1) helped it transfer from chloroform to water layer. However, Duan et al.¹⁴ reported that the amphiphilic nanocrystal/PDMAEMA nanoparticles do not show a phase transfer from chloroform to water phase.

Temperature- and pH-Dependent Solubility. It has been known that PDMAEMA shows a LCST of $\sim 45^\circ\text{C}$.¹⁶ Thus, the molecular chain of PDMAEMA is fully extended below 45°C and entangled above 45°C. Figure 8(a) shows a temperature-dependent solubility of PDMAEMA-functionalized MWNT. The aqueous solution of PDMAEMA-functionalized MWNT showed a stable dispersion at 20°C and a precipitation at 80°C. Such an observation of temperature-dependent solubility supports that the PDMAEMA-functionalized MWNT shows a LCST behavior. Figure 8(b) shows a solubility of the PDMAEMA-functionalized MWNT depending on the pH value of aqueous solution. The PDMAEMA-functionalized MWNT shows a stable aqueous solution at pH 8 and 12, while it is precipitated at pH 3. The aggregation of PDMAEMA-functionalized MWNT in the acidic

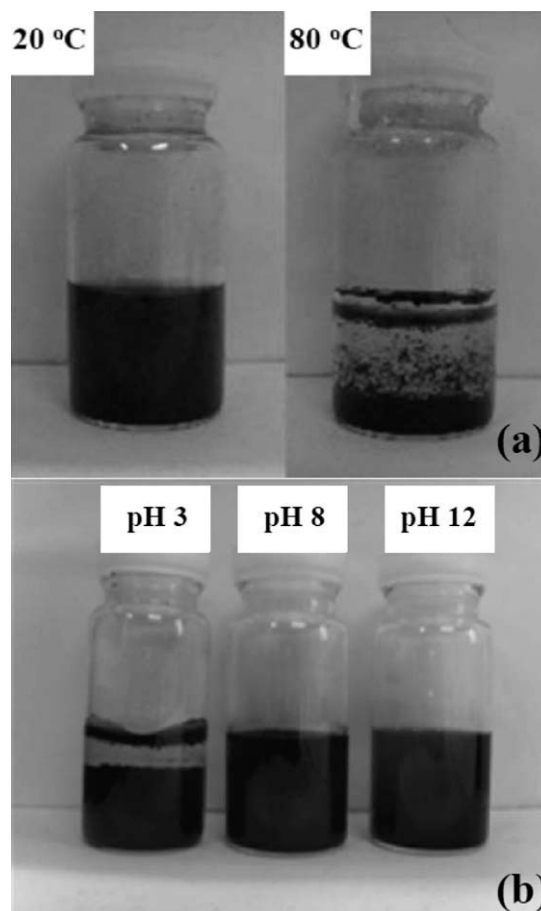


Figure 8. (a) Temperature- and (b) pH-dependent solubility for the PDMAEMA-functionalized MWNT (Cu(I)Br/PMDETA and 60°C in ATRP; PDMAEMA 53.9 wt %).

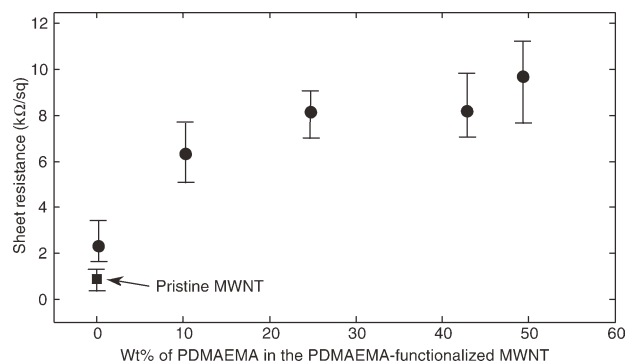


Figure 9. Sheet resistance depending on the wt % of PDMAEMA present in the PDMAEMA-functionalized MWNT (Cu(I)Br/PMDETA and 60°C in ATRP).

environment (pH 3) contradicts the report by Hu et al.,¹⁸ in which they observed that the PDMAEMA-grafted CNTs are soluble in a pH 2 solution and is aggregated in a pH 11 solution. The tertiary amine of the PDMAEMA is partially protonated in neutral pH and entirely protonated in an acidic environment, and thus the tertiary amine gets a proton to form quaternary ammonium.¹⁷ However, it is noted that there remains the acid (—COOH) group in the PDMAEMA-functionalized MWNT prepared in this study. It is probable that in the acidic solution of pH 3, the interactions between the protonated PDMAEMA chains and the acid group present in the surface of MWNT are stronger than the polymer chain–solvent interactions. Thus, the PDMAEMA-functionalized MWNT prepared in this study shows a precipitation at a pH 3 solution.

Sheet Resistance. Sheet resistance for the PDMAEMA-functionalized MWNT was measured to confirm its electrical conductivity, and the results are shown in Figure 9. The sheet resistance of pristine MWNT used in this study was measured to be $\sim 0.861 \times 10^3 \Omega/\text{sq}$, which is quite high due to the presence of CMC (<5 wt %) contained in the specimen and that of the PDMAEMA-functionalized MWNT was increased up to $\sim 9.68 \times 10^3 \Omega/\text{sq}$ at the polymer content of 53.9 wt % PDMAEMA. The potential applications of PDMAEMA-functionalized MWNT prepared in this study are the EMI shielding and ESD areas with the desired surface resistance ranging from 10^2 to $10^8 \Omega/\text{sq}$.

Antibacterial Effect of the Quaternization-Treated PDMAEMA-Functionalized MWNT. PDMAEMA shows antibacterial effect against Gram-negative and Gram-positive bacteria due to the presence of cation moiety generated after quaternization. According to Rawlinson et al.,¹³ the mode of action for cationic biocides is as follows. The positively charged PDMAEMA is adsorbed onto the surface of bacterial cell by the electrostatic interaction. Then, the polymer diffuses through the cell wall, binds to cytoplasmic membrane, and destroys the membrane. Finally, cytoplasmic constituents are released, and the cell is to be dead.

Figure 10 shows the SEM microphotographs of cultured *E. coli* present in both a pristine cellulose filter paper without any treatment and a cellulose filter paper coated with the quaternization-treated PDMAEMA-functionalized MWNT. Figure 10(a)

shows that *E. coli* maintains its original cylindrical structure in the blank sample, while in the treated sample, the cell membranes of *E. coli* were destroyed and transformed from cylindrical to planar structure [Figure 10(b)]. This experimental observation supports that cell death occurs in the quaternization-treated PDMAEMA-functionalized MWNT, and it is caused by the disruption of cytoplasmic membrane of *E. coli*. Figure 11 shows the colony images of *E. coli* cultured in the agar plate containing nothing, pristine MWNT, and the quaternization-treated PDMAEMA-functionalized MWNT. The number of CFU for blank sample is 401, 352 for the pristine MWNT, and 231–359 for the quaternization-treated PDMAEMA-functionalized MWNT. The CFU data of samples based on cultured *E. coli* in agar plate are summarized in Table II. The antibacterial effect can be quantitatively compared by estimating the loss of viability of *E. coli*, which is calculated as follows:

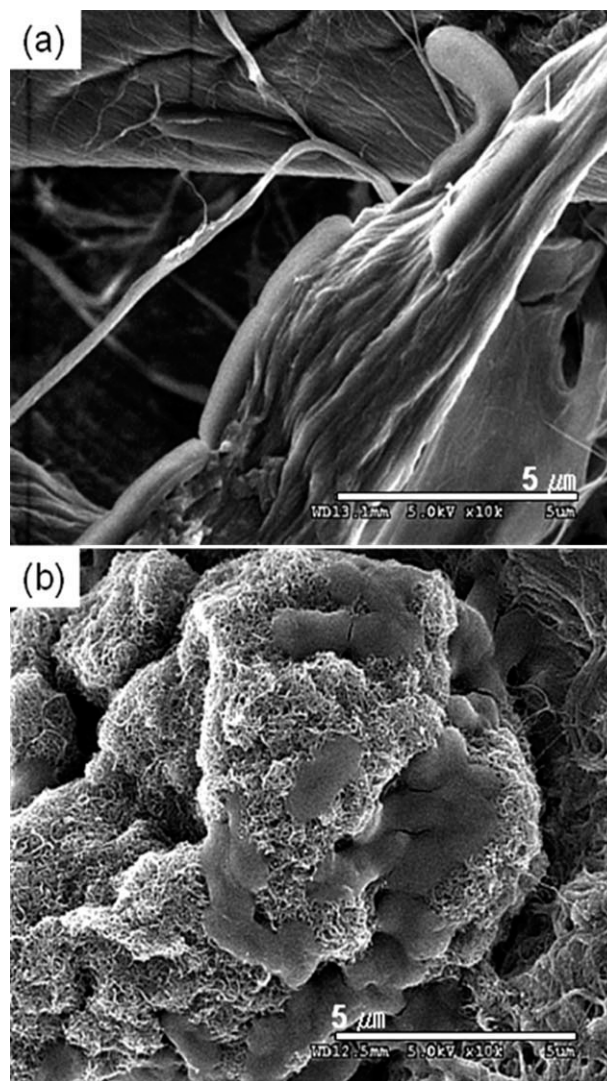


Figure 10. SEM microphotographs of cultured *E. coli* present in (a) a pristine filter paper without any treatment and (b) a filter paper coated with the quaternization-treated PDMAEMA-functionalized MWNT (Cu(I)Br/PMDETA and 60°C in ATRP; PDMAEMA 53.9 wt %) (b).

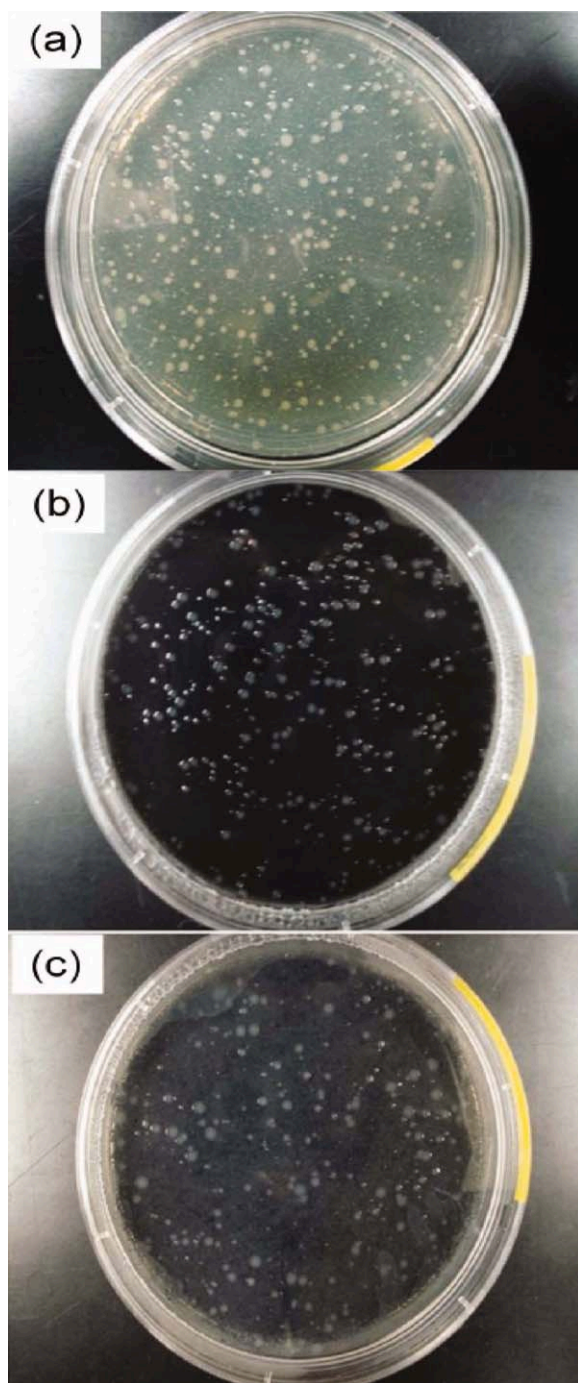


Figure 11. Colony images of *E. coli* cultured in the agar plate containing (a) nothing, (b) pristine MWNTs, and (c) the quaternization-treated PDMAEMA-functionalized MWNT (Cu(I)Br/PMDETA and 60°C in ATRP; PDMAEMA 53.9 wt %). [Color figure can be viewed in the online issue, which is available at wileyonlinelibrary.com.]

$$\text{Loss of viability (\%)} = \frac{(\text{CFU of Blank}) - (\text{CFU of nanocomposites})}{(\text{CFU of Blank})} \times 100 \quad (2)$$

Figure 12 shows the loss of viability of *E. coli* depending on the wt % of PDMAEMA in the PDMAEMA-functionalized

Table II. CFU Data Based on the Cultured *E. coli* in Agar Plate

Sample	Copper complex	CFU
Blank		401 ± 16
MWNT		352 ± 7
TPMA	Cu(I)Br	262 ± 11
dNbpy	Cu(I)Br	337 ± 14
Bpy	Cu(I)Br	359 ± 8
Bpy	Cu(I)Cl	277 ± 11
PMDETA	Cu(I)Br	231 ± 8

MWNT prepared by applying the combination of various types of ligands and copper complex of either Cu(I)Br or Cu(I)Cl at 60°C in ATRP. The loss of viability of *E. coli* is highly affected by the PDMAEMA content in the quaternization-treated PDMAEMA-functionalized MWNT, and the highest viability loss was achieved at ~ 42% with the PDMAEMA-functionalized MWNT-containing 53.9 wt % of PDMAEMA [Cu(I)Br/PMDETA and 60°C in ATRP]. It reveals that the loss of viability of *E. coli* is proportional to the wt % of PDMAEMA in the PDMAEMA-functionalized MWNT. Roy et al.³² reported that PDMAEMA grafted onto a cellulose filter paper shows an antibacterial activity against *E. coli* and cellulose-*g*-PDMAEMA having high-grafting ratio shows much increased loss of viability of *E. coli*. An antibacterial activity of pristine MWNT against *E. coli* was estimated with the loss of viability of ~ 12%, which is known to be caused by the nanosized structure of MWNT.^{3,4} The presence of PDMAEMA grafted onto the surface of MWNT is a prevailing cause for the antibacterial effect of PDMAEMA-functionalized MWNT.

An antibacterial activity against *S. aureus* was observed for the PDMAEMA-functionalized MWNT. Figure 13 shows the colony images of *S. aureus* cultured in the agar plate containing nothing and the quaternization-treated PDMAEMA-functionalized MWNT. The number of CFU for blank sample is too many to count, while that for the quaternization-treated PDMAEMA-functionalized MWNT is very few.

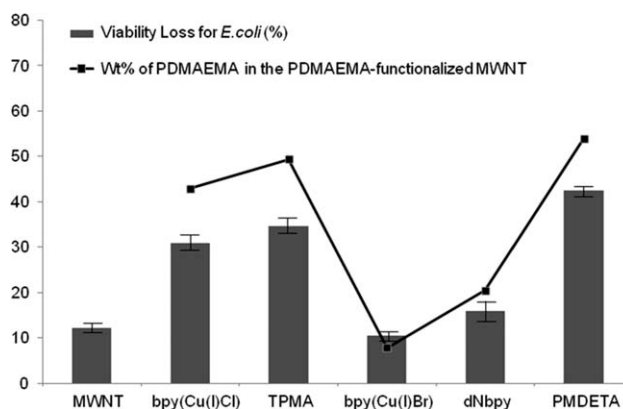


Figure 12. Loss of viability of *E. coli* depending on the wt % of PDMAEMA in the PDMAEMA-functionalized MWNT (Cu(I)Br) in case of unspecifying and 60°C in ATRP.

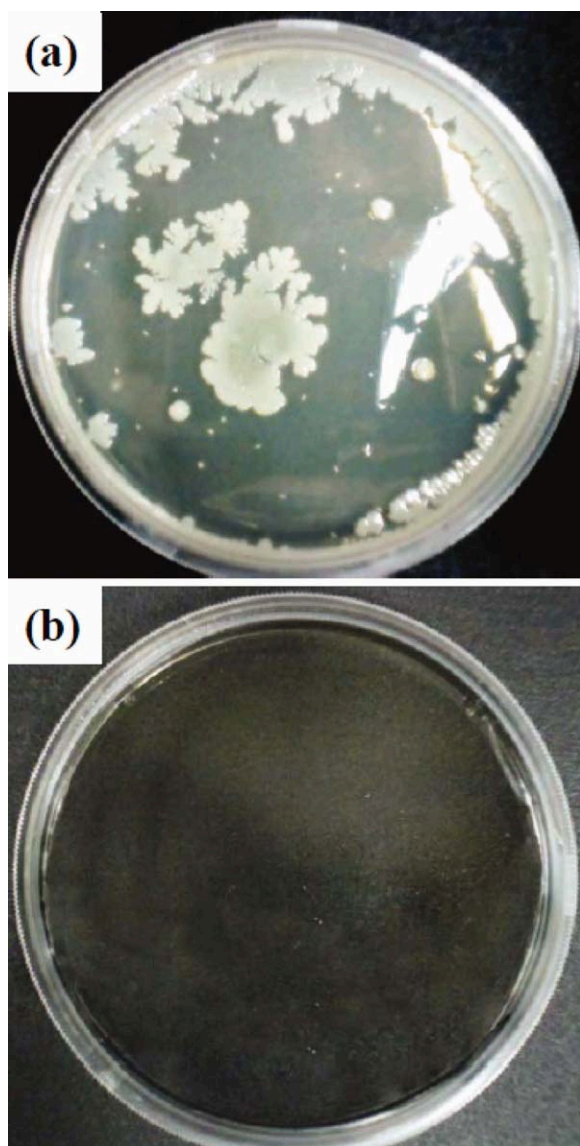


Figure 13. Colony images of *S. aureus* cultured in the agar plate containing (a) nothing and (b) the quaternization-treated PDMAEMA-functionalized MWNT (Cu(I)Br/PMDETA and 60°C in ATRP; PDMAEMA 53.9 wt %). [Color figure can be viewed in the online issue, which is available at wileyonlinelibrary.com.]

CONCLUSIONS

The PDMAEMA-functionalized MWNT was successfully prepared by applying the “grafting-from” method as a chemical strategy for grafting polymer onto MWNT, which is an ATRP of DMAEMA using the bromine-functionalized MWNT (MWNT-Br) as an initiator. PDMAEMA grafted onto the functionalized MWNT was identified by the spectroscopic analysis such as FTIR and Raman, and it was shown that all the analysis results carried out in this study support that PDMAEMA is covalently anchored to the MWNT. The linear relationship between polymer content in the PDMAEMA-functionalized MWNT and Raman relative intensity ratio of D to G band (I_D/I_G) confirmed the formation of sp^3 -hybridized carbons on the PDMAEMA-

grafted MWNT, and such a relationship can be used as a tool for a measure of the degree of functionalization of MWNT.

The PDMAEMA content in the PDMAEMA-functionalized MWNT was estimated by applying the correlation equation based on the thermal weight loss values (wt %) at 800°C in the TGA thermogram regarding MWNT-Br, PDMAEMA, and the PDMAEMA-functionalized MWNT. The living controlled free radical polymerization, which is ATRP in this study, was characterized by the confirmation of linearity between the PDMAEMA content in the PDMAEMA-functionalized MWNT and the amount of DMAEMA based on the weight of MWNT-Br used in ATRP. It was shown that the PDMAEMA composition in the PDMAEMA-functionalized MWNT depends on the type of copper complex and ligand, the rate constant value of ATRP activation path for ligand, and the ATRP temperature.

The PDMAEMA-functionalized MWNT showed solubility in water as well as organic solvents confirming an amphipathic nature. The solubility of PDMAEMA-functionalized MWNT in water showed not only a LCST behavior but also a dual responsive property of temperature and pH value. The quaternization-treated PDMAEMA-functionalized MWNT clearly showed an antibacterial effect against *E. coli* as well as *S. aureus*. It was shown that the loss of viability of *E. coli* highly depends on the PDMAEMA content in the PDMAEMA-functionalized MWNT, and the highest viability loss achieved in this study was ~ 42% with the PDMAEMA-functionalized MWNT containing 53.9 wt % of PDMAEMA. The PDMAEMA-functionalized MWNT prepared in this study showed sheet resistance less than $\sim 9.68 \times 10^3 \Omega/\text{sq}$. Therefore, the authors suggest that the PDMAEMA-functionalized MWNT can be applied for the EMI shielding or ESD area requiring for not only the antibacterial effect against Gram-negative and Gram-positive bacteria but also the mechanical reinforcements.

ACKNOWLEDGMENTS

This work was supported by Basic Science Research Program through the National Research Foundation of Korea (NRF) funded by the Ministry of Education, Science and Technology (2011-0027056).

REFERENCES

- Spitalsky, Z.; Tasis, D.; Papagelis, K.; Galiotis, C. *Prog. Polym. Sci.* **2010**, *35*, 357.
- Homenick, C. M.; Lawson, G.; Adronov, A. *Polym. Rev.* **2007**, *47*, 265.
- Kang, S.; Pinault, M.; Pfefferle, L. D.; Elimelech, M. *Langmuir.* **2007**, *23*, 8670.
- Kang, S.; Herzberg, M.; Rodrigues, D. F.; Elimelech, M. *Langmuir.* **2008**, *24*, 6409.
- Brady-Estévez, A. S.; Schnoor, M. H.; Kang, S.; Elimelech, M. *Langmuir.* **2010**, *26*, 19153.
- Zhou, J.; Qi, X. *Lett. Appl. Microbiol.* **2011**, *52*, 76.

7. Pangule, R. C.; Brooks, S. J.; Dinu, C. Z.; Bale, S. S.; Salmon, S. L.; Zhu, G.; Metzger, D. W.; Kane, R. S.; Dordick, J. S. *ACS. Nano.* **2010**, *4*, 3993.
8. Wu, C. *Carbon* **2009**, *47*, 3091.
9. Timofeeva, L.; Kleshcheva, N. *Appl. Microbiol. Biotechnol.* **2011**, *89*, 475.
10. Green, J. D.; Bickner, S.; Carter, P. W.; Fulghum, T.; Luebke, M.; Nordhaus, M. A.; Strathmann, S. *Biotechnol. Bioeng.* **2011**, *108*, 231.
11. Wang, H.; Wang, L.; Zhang, P.; Yuan, L.; Yu, Q.; Chen, H. *Colloid. Surf B: Biointerf.* **2011**, *83*, 355.
12. Rawlinson, L. B.; O'Brien, P. J.; Brayden, D. J. *J. Control Release* **2010**, *146*, 84.
13. Rawlinson, L. B.; Ryan, S. M.; Mantovani, G.; Syrett, J. A.; Haddleton, D. M.; Brayden, D. J. *Biomacromolecules* **2010**, *11*, 443.
14. Duan, H.; Kuang, M.; Wang, D.; Kurth, D. G.; Möhwald, H. *Angew. Chem. Int. Ed.* **2005**, *44*, 1717.
15. Schepelina, O.; Zharov, I. *Langmuir.* **2008**, *24*, 14188.
16. Dai, S.; Ravi, P.; Tan, C. H.; Tam, K. C. *Langmuir.* **2004**, *20*, 8569.
17. Zhou, L.; Yuan, W.; Yuan, J.; Hong, X. *Mater. Lett.* **2008**, *62*, 1372.
18. Hu, H.; Yu, B.; Ye, Q.; Gu, Y.; Zhou, F. *Carbon.* **2010**, *48*, 2347.
19. Priftis, D.; Sakellariou, G.; Mays, J. W.; Hadjichristidis, N. *J. Polym. Sci. Part A Polym. Chem.* **2010**, *48*, 1104.
20. Gao, C.; Li, W.; Morimoto, H.; Nagaoka, Y.; Maekawa, T. *J. Phys. Chem. B* **2006**, *110*, 7213.
21. Li, W.; Gao, C.; Qian, H.; Ren, J.; Yan, D. *J. Mater. Chem.* **2006**, *16*, 1852.
22. Meyer, F.; Minoia, A.; Raquez, J. M.; Spasova, M.; Lazzaroni, R.; Dubois, P. *J. Mater. Chem.* **2010**, *20*, 6873.
23. Kong, H.; Luo, P.; Gao, C.; Yan, D. *Polymer* **2005**, *46*, 2472.
24. Kong, H.; Gao, C.; Yan, D. *J. Am. Chem. Soc.* **2004**, *126*, 412.
25. Joo, Y. T.; Jin, S. M.; Kim, Y. *Polymer (Korea)* **2009**, *33*, 452.
26. Yang, Y.; Wang, J.; Zhang, J.; Liu, J.; Yang, X.; Zhao, H. *Langmuir.* **2009**, *25*, 11808.
27. Wang, S.; Jiang, S. P.; Wang, X. *Nanotechnology* **2008**, *19*, 265601.
28. Liu, Y.; Chang, Y.; Liang, M. *Polymer* **2008**, *49*, 5405.
29. Gao, C.; Jin, Y. Z.; Kong, H.; Whitby, R. L. D.; Acquah, S. F. A.; Chen, G. Y.; Qian, H.; Hartschuh, A.; Silva, S. R. P.; Henley, S.; Fearon, P.; Kroto, H. W.; Walton, D. R. M. *J. Phys. Chem. B* **2005**, *109*, 11925.
30. Bahr, J. L.; Tour, J. M. *Chem. Mater.* **2001**, *13*, 3823.
31. Tang, W.; Matyjaszewski, K. *Macromolecules* **2006**, *39*, 4953.
32. Roy, D.; Knapp, J. S.; Guthrie, J. T.; Perrier, S. *Biomacromolecules* **2008**, *9*, 91.